ORIGINAL ARTICLE

Molecular imaging with ^{68}Ga-SSTR PET/CT and correlation to immunohistochemistry of somatostatin receptors in neuroendocrine tumours

Daniel Kaemmerer · Luisa Peter · Amelie Lupp · Stefan Schulz · Jörg Sänger · Vikas Prasad · Harshad Kulkarni · Sven-Petter Haugvik · Merten Hommann · Richard Paul Baum

Abstract

Purpose Somatostatin receptors (SSTR) are known for an overexpression in gastroenteropancreatic neuroendocrine tumours (GEP-NET). The aim of the present study was to find out if the receptor density predicted by the semi-quantitative parameters generated from the static positron emission tomography (PET/CT) correlated with the in vitro immunohistochemistry using a novel rabbit monoclonal anti-SSTR2A antibody (clone UMB-1) for specific SSTR2A immunohistochemistry and polyclonal antibodies for SSTR1 and 3–5.

Methods Overall 14 surgical specimens generated from 34 histologically documented GEP-NET patients were correlated with the preoperative ^{68}Ga-DOTA-NOC PET/CT.

Quantitative assessment of the receptor density was done using the immunoreactive score (IRS) of Remmele and Stegner; the additional 4-point IRS classification for immunohistochemistry and standardized uptake values (SUV$_{max}$ and SUV$_{mean}$) were used for PET/CT.

Results The IRS for SSTR2A and SSTR5 correlated highly significant with the SUV$_{max}$ on the PET/CT ($p<0.001$; $p<0.05$) and the IRS for SSTR2A with the SUV$_{mean}$ ($p<0.013$). The level of SSTR2A score correlated significantly with chromogranin A staining and indirectly to the tumour grading.

Conclusion The highly significant correlation between SSTR2A and SSTR5 and the SUV$_{max}$ on the ^{68}Ga-DOTA-NOC PET/CT scans is concordant with the affinity profile of ^{68}Ga-DOTA-NOC to the SSTR subtypes and demonstrates the excellent qualification of somatostatin analogues in the diagnostics of NET. This study correlating somatostatin receptor imaging using ^{68}Ga-DOTA-NOC PET/CT with immunohistochemically analysed SSTR also underlines the approval of therapy using somatostatin analogues, follow-up imaging as well as radionuclide therapy.

Both authors contributed equally to the manuscript.

D. Kaemmerer (✉) · S.-P. Haugvik · M. Hommann
Department of General and Visceral Surgery,
Zentralklinik Bad Berka GmbH,
Robert-Koch-Allee 9,
99437 Bad Berka, Germany
e-mail: Daniel.Kaemmerer@zentralklinik.de

L. Peter · A. Lupp · S. Schulz
Department of Pharmacology and Toxicology,
University of Jena,
Jena, Germany

J. Sänger
Laboratory of Pathology and Cytology,
Bad Berka, Germany

V. Prasad · H. Kulkarni · R. P. Baum
Department of Nuclear Medicine and Center for PET,
Zentralklinik Bad Berka,
Bad Berka, Germany

Introduction

Gastroenteropancreatic neuroendocrine tumours (GEP-NET) are known for an overexpression of somatostatin receptors (SSTR), which already serves as a molecular basis for different methods of diagnostics and therapies

[e.g. in vivo diagnostics and peptide receptor radionuclide therapies (PRRT)], and realizes a prognostic estimation of the malignant disease [1]. So far, six subtypes of SSTR have been identified: SSTR1, 2A, 2B, 3, 4 and 5 [2]. Among the subtypes, 2A and 2B are so-called splice variants, and only the 2A variant has been identified in human tissue [3]. In order to estimate the prognosis of GEP-NET in a patient with an SSTR-positive tumour, the density, distribution and subtype profile of the SSTR have to be determined. SSTR2A is expressed most frequently, followed by SSTR1 and 5 and rarely SSTR3 and 4 [4]. SSTR2A is a membrane-bound receptor, whereas SSTR1, 3 and 5 are located intracellularly [5]. In the diagnostics of NET, positron emission tomography/computed tomography (PET/CT) using SST analogues like DOTA-TOC, DOTA-NOC or DOTA-TATE labelled with positron-emitting radionuclides (e.g. ^{68}Ga, ^{64}Cu) has shown a higher sensitivity and specificity as compared to SSTR scintigraphy [6]. Because of its high sensitivity and tumour contrast along with a high image quality as early as 30 min after injection, ^{68}Ga-labelled SSTR PET/CT is currently the most preferred radiological technique in the diagnostics of NET [7]. Several studies have shown the advantage of ^{68}Ga-DOTA-TOC as compared to ^{111}In-octreotide single photon emission computed tomography (SPECT) [8]. While in 2004 Baum and Hoffmann described ^{68}Ga-DOTA-TOC PET/CT as the most sensitive method in diagnosing NET, Antunes et al. later showed an advantage of ^{68}Ga-DOTA-NOC over ^{68}Ga-DOTA-TOC [9]. The high expression of SSTR in neuroendocrine tumour cells not only serves as a target in the diagnostics of NET (e.g. SSTR scintigraphy, SSTR PET/CT), but also enables the development of new therapeutic approaches like PRRT, a specifically targeted therapy of increasing importance. In PRRT radionuclides bind specifically to SSTR. Studies have shown that PRRT can lead to a tumour reduction of about 50% in about a quarter of the patients treated, with only a minority of severe side effects [10]. This radioactive labelling allows internal radiotherapy with protection of the non-affected tissue and therefore allows therapy of disseminated metastases.

The aim of this study was to clarify if there was a correlation between SSTR PET/CT, using the standardized uptake value (SUV) as a parameter of the SSTR density in GEP-NET and/or its metastases, and the expression intensity of the five SSTR subtypes in surgically removed GEP-NET tissue, which can be evaluated by immunohistochemical analysis. Therefore, a second aim of this study was to exactly quantify the SSTR distribution of all five SSTR subtypes in different GEP-NET using immunohistochemical analysis and through this to allow for a general statement on the

effectiveness of therapy with somatostatin analogues and also to allow for a correlation with SSTR PET/CT. A further aim of this study was to evaluate a possible relationship between clinical and histopathological traits in GEP-NET and SSTR status.

Materials and methods

A total of 44 tumour samples obtained both from primary tumours and from metastases from 34 patients with GEP-NET were analysed for SSTR1–5. The samples were embedded in paraffin and sections with a thickness of 4 μm were prepared using a microtome. The sections were then transferred to a microscope slide and air-dried. Immunohistochemical analysis was performed on all tumour samples (Fig. 1).

Immunohistochemistry

The detection of SSTR subtypes was performed using the labelled streptavidin-biotin method (LSAB) and counterstaining was done with haematoxylin. The peptides used
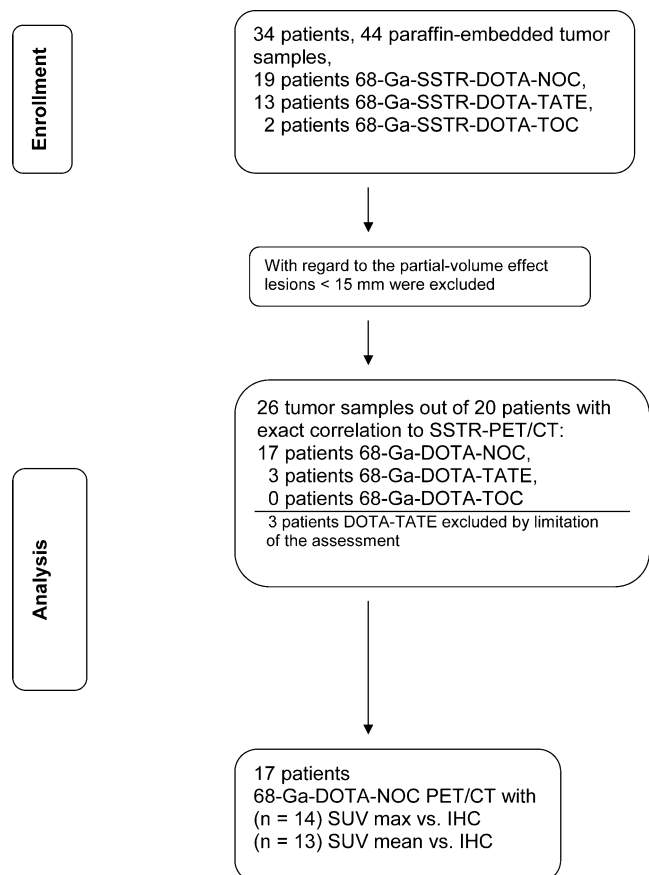

Fig. 1 Flowchart of patients and tumour specimens which were correlated to SSTR PET/CT

for detection of SSTR2A were produced by Epitomics (Burlingame, CA, USA) and for detection of SSTR1, 3, 4 and 5 by Gramsch Laboratories (Schwabhausen, Germany). The semi-quantitative analysis of the stained sections was done with light microscopy according to the immunoreactive score (IRS) by Remmele and Stegner. The IRS evaluation in this study was based on a modification by McCarty et al. in 1985, which not only evaluates the visualized grade of colour intensity (staining), but also adds the fraction of cells in each intensity category [11]. The IRS with points 0–12 was adapted to an additional 4-point IRS classification (Table 1, Fig. 2). The immunohistochemical analysis was performed by two independent investigators on each tissue section.

Imaging

The exact location of the tumour was defined by preoperative ^{68}Ga-SSTR PET/CT scans in combination with surgery and pathology protocols. The SUV_{max} and SUV_{mean} were measured. The PET/CT scans were processed with Siemens e.soft Nuclear Medicine Workstation. All other clinical data were gathered from the patient records. Considering the partial volume effect for lesions <1.5 cm, 14 cases were evaluated for SUV_{max}, whereas 13 cases were evaluated for SUV_{mean}, using ^{68}Ga-DOTA-NOC PET/CT scans (Fig. 1). Because of the limitations in the assessment of the partial volume effect, only three cases in the DOTA-TATE group were left, which were then excluded from the analysis.

Statistics

Data were analysed using SPSS for Windows 15.0. The following parameters were normally distributed according to the Kolmogorov-Smirnov test: body mass, age, body mass index (BMI), IRS, SSTR1, 3 and 5, SUV_{max} and SUV_{mean}. All other variables were not normally distributed. After assessment of normal distribution, the following tests were used: Kruskal-Wallis test, χ^2 test, Fisher's exact test, Kendall's tau correlation analysis and Spearman's rank correlation analysis.

Results

Patient data

Of the 34 patients included in the study, 44 different tumour samples were processed as paraffin-embedded blocks. A corresponding localization of tumour tissue on preoperative PET/CT scans with ^{68}Ga-DOTA-NOC or ^{68}Ga-DOTA-TATE was found in 26 of 44 (59.1%) of the tumour samples (Figs. 3 and 4). ^{68}Ga-DOTA-NOC and corresponding immunohistochemical correlations could be performed in 17 patients (SUV_{max} n=17, SUV_{mean} n=13 patients; Fig. 1, Table 2). The median age of the patients at the time of surgery was 58 years (range 33–82 years).

Tumour localization

The organs of tumour localization in decreasing order of frequency were the pancreas with 35.3% (n=12) and the ileum with 29.4% (n=10), followed by cancer of unknown primary (CUP) in 14.7% (n=5), stomach in 8.8% (n=3), other tumours in 8.8% (n=3) and appendix in 2.9% (n=1) of the tumours. Hepatic metastases were present in 64.7% (n=22) and peritoneal carcinosis in 32.4% (n=11). According to the TNM classification, 58.8% (n=20) of the patients in the study showed a T4 stage, 70.6% (n=24) had a positive lymph node status and 82.4% (n=28) had an M1 stage.

Grading

Of the patients, 64.7% (n=22) had a moderately differentiated (G2), 20.6% (n=7) a well-differentiated (G1) and 14.7% (n=5) a poorly differentiated tumour tissue (G3).

Immunohistochemistry

Chromogranin A and synaptophysin

Of the patients, 82.4% (n=28) had tumour tissue positive for chromogranin A, 8.8% (n=3) showed only a light

Table 1 Immunoreactive score (IRS) and IRS classification

Percentage of positive cells	X Intensity of staining	= IRS (0–12)	IRS classification
0 = no positive cells	0 = no colour reaction	0–1 = negative	0 = negative
1 = < 10% of positive cells	1 = mild reaction	2–3 = mild	1 = positive, weak expression
2 = 10–50% positive cells	2 = moderate reaction	4–8 = moderate	2 = positive, mild expression
3 = 51–80% positive cells	3 = intense reaction	9–12 = strongly positive	3 = positive, strong expression
4 = > 80% positive cells			

Fig. 2 Immunohistochemical localization of SSTR1–5 (*red*). **a** Lymph node metastasis. **b** Neuroendocrine carcinoma of the terminal ileum. **c** Neuroendocrine carcinoma of the pancreas head. **a** SSTR1: IRS=2 points (IRS classification: 1); SSTR2A: IRS=9 points (IRS classification: 3); SSTR3: IRS=9 points (IRS classification: 3); SSTR4: IRS=4 points (IRS classification: 2); SSTR5: IRS=2 points (IRS classification: 1). **b** SSTR1: IRS=0 points (IRS classification: 0); SSTR2A: IRS=4.5 points (IRS classification: 2); SSTR3: IRS=4.5 points (IRS classification: 2); SSTR4: IRS=2 points (IRS classification: 1); SSTR5: IRS=2 points (IRS classification: 1). **c** SSTR1: IRS=6 points (IRS classification: 2); SSTR2A: IRS=12 points (IRS classification: 3); SSTR3: IRS=12 points (IRS classification: 3); SSTR4: IRS=6 points (IRS classification: 2); SSTR5: IRS=6 points (IRS classification: 2)
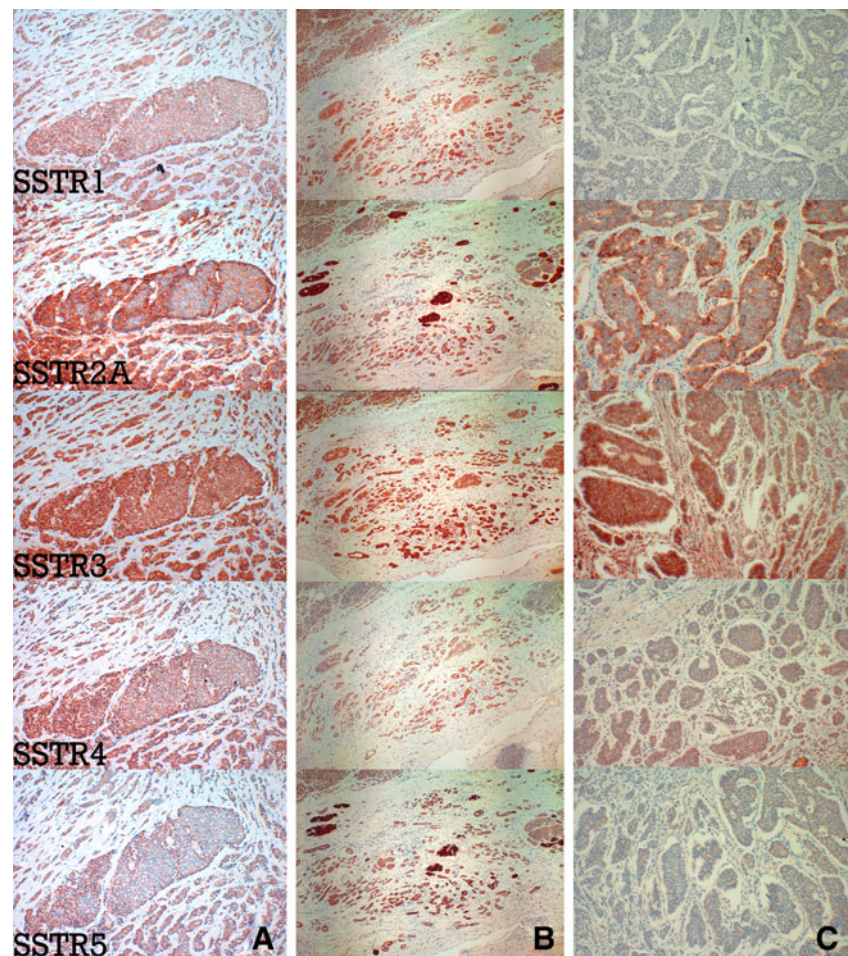
chromogranin staining and another 8.8% (*n*=3) showed no chromogranin staining at all; 82.4% of the patients (*n*=28) had tumour tissue positive for synaptophysin, another 8.8% (*n*=3) showed a slight synaptophysin staining and no staining was seen in 2.9% (*n*=1). In 5.9% of the patients (*n*=2) the synaptophysin staining was not specified.

Ki-67 index

In 41 specimens the Ki-67 index was assigned. In 17.1% of the specimens (*n*=7) the Ki-67 was ≤2%, in 53.7% (*n*=22) between 2 and 10% and in 29.3% (*n*=12)>10%.

SSTR expression pattern

The IRS yielded 16 different expression patterns depending on the predominance of positive staining for SSTR1, 2A, 3 or 5. In 81.8% of the paraffin block specimens (*n*=36), at least SSTR2A and 3 were positive, SSTR1, 2A and 3 were positive in 43.2% (*n*=19) and in 70.5% (*n*=31) at least

three of the subtypes showed a positive staining. None of the sections was completely negative for all five SSTR subtypes according to the IRS.

Distribution of the positive SSTR subtypes

The presence of an SSTR subtype was defined as positive if the IRS classification was ≥2. All tumours with a value of <2 were defined as negative for the specific SSTR. According to the IRS classification, the most common subtype was SSTR3 followed by SSTR2A > SSTR4 > SSTR1 > SSTR5 (Table 3).

Immunohistochemistry and clinical data localization

Scores versus grading

There was a significant inverse correlation between the IRS classification of the SSTR2A and the grading of the tumour samples (primaries and metastases) according to Fisher's exact test (*p*<0.005). The IRS did not show any significant
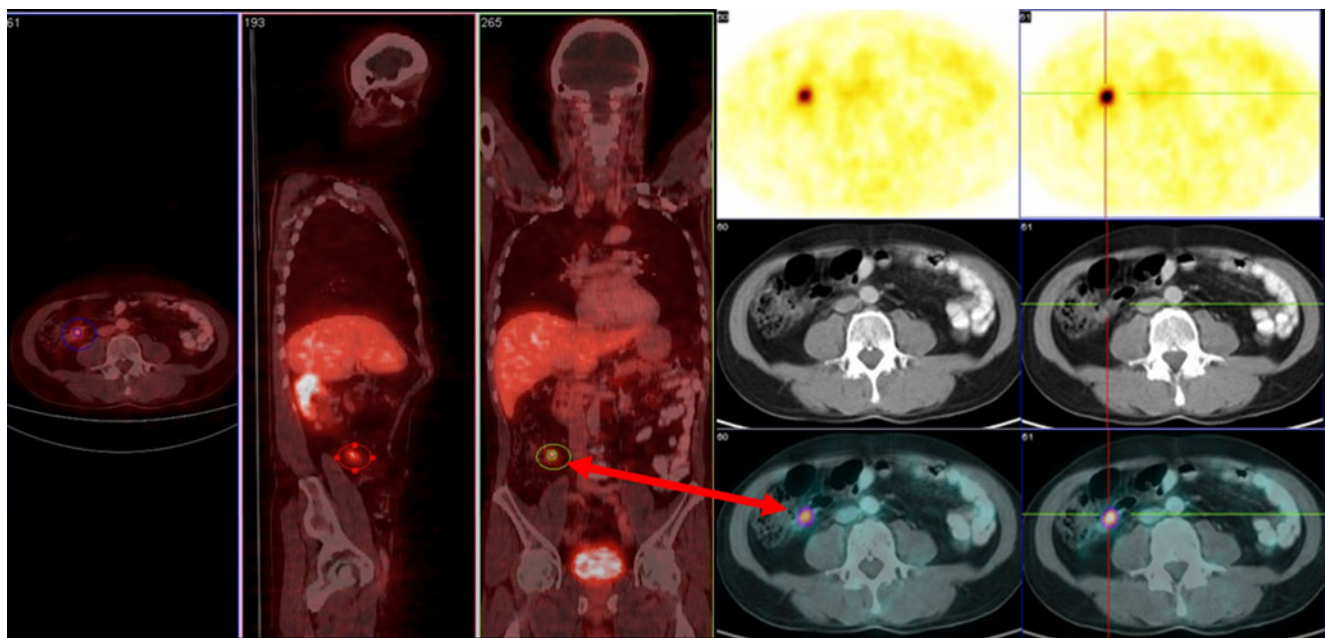
Fig. 3 SSTR PET/CT patient 1: neuroendocrine carcinoma of the terminal ileum pT2 pN1 pM1 (G2), stage IV, labelled primary of the ileum with SUV_{max} 8.3, pathological size 1.5 cm coherent to the immunohistochemical images (Fig. 2b)

correlation (p=0.12). In a subgroup analysis of the tumour tissues separated into primaries and metastases there was no significant correlation between IRS/IRS classification and grading detectable.

Scores versus chromogranin A

The IRS and the IRS classification of the SSTR2A correlated significantly with the intensity of the chro-
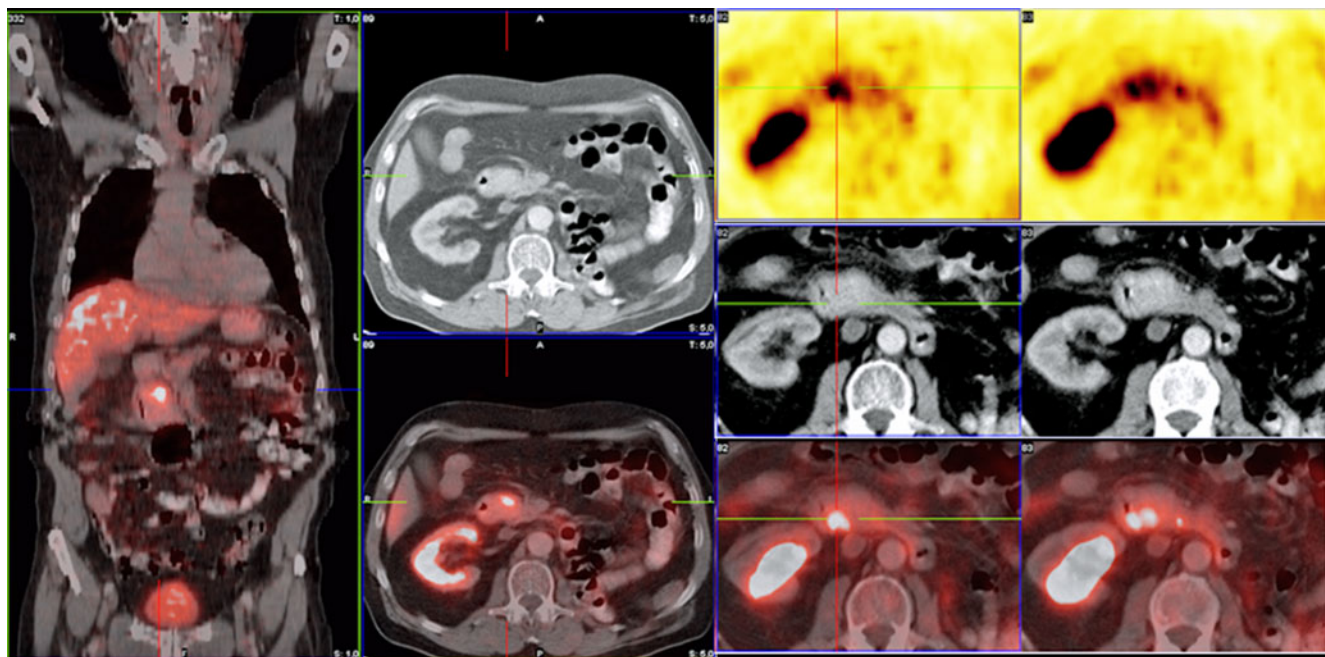

Fig. 4 SSTR PET/CT patient 2: neuroendocrine carcinoma of the pancreas head pT3 pN1 pM1 (G2), stage IV, labelled primary of the pancreas head with SUV_{max} 10.5, pathological size 3.5 cm coherent to the immunohistochemical images (Fig. 2c)

Table 2 Patients' baseline characteristics who underwent ^{68}Ga-DOTA-NOC PET/CT

No.	Primary	WHO 2010 classification	Stage
1	Ileum	NET G2	IV
2	Duodenum	NET G2	IV
3	Appendix	NEC G3	IV
4	Ovary	NET G2	IV
5	Ileum	NET G2	IV
6	Ileum	NET G2	IV
7	Stomach	NEC G3	IV
8	Ileum	NET G2	IV
9	Ileum	NET G2	IV
10	Ileum	NET G2	IV
11	Pancreas	NET G2	IV
12	Pancreas	NET G2	IV
13	Pancreas	NET G2	IV
14	Pancreas	NET G2	IV
15	Stomach	NET G2	IV
16	Pancreas	NEC G3	IV
17	Ileum	NET G1	IV

mogranin staining, IRS 0.3 (p=0.002) and IRS classification 0.24 (p=0.008). For the other SSTR subtypes a significant correlation could not be shown.

Immunohistochemistry and SSTR PET/CT

Score versus SUV$_{max}$/SUV$_{mean}$

The SUV$_{max}$ ranged from 5.7 to 33.7. There was no significant correlation between the immunohistochemical score (IRS) of SSTR1, 3 and 4 and the variable SUV$_{max}$ ($0.3 < p < 0.8$). However, the correlation between the IRS of SSTR2A and SUV$_{max}$ and the IRS of SSTR5 and SUV$_{max}$, respectively, were highly significant (SSTR2A $p < 0.001$; SSTR5 $p < 0.04$). The IRS classification correlated with SUV$_{max}$. A significant value was not detectable ($0.14 < p < 0.8$). A statistically significant correlation between the SUV$_{mean}$ and the IRS of SSTR1, 3, 4 and 5 was not seen.

The IRS and SUV$_{mean}$ correlated significantly ($p < 0.01$) with SSTR2A. The IRS classification could not be associated significantly to the SSTR subtypes ($0.16 < p < 0.70$).

Discussion

The aim of this study was to clarify whether there was a correlation between the intensity of expression of the five SSTR subtypes, measured with immunohistochemical analysis on surgically removed tumour tissue, and the SSTR density of these tumours, using SUV measured in

Table 3 SSTR subtype distribution and frequencies classified according to scores (IRS and IRS classification)

IRS SSTR-subtype	IRS classification SSTR-subtype
IRS SSTR1	IRS classification SSTR1
Score/frequency (%)	Score/frequency (%)
0/7 (15.9)	0/7 (15.9)
2/8 (18.2)	1/16 (36.4)
3/4 (9.1)	2/21 (47.7)
3.5/4 (9.1)	
4/15 (34.1)	
6/6 (13.6)	
SSTR1 positive total	21 (47.7%)
IRS SSTR2A	IRS classification SSTR2A
Score/frequency (%)	Score/frequency (%)
2/2 (4.5)	1/6 (13.6)
3/4 (9.1)	2/20 (45.5)
4/5 (11.4)	3/18 (40.9)
4.5/2 (4.5)	
5/1 (2.3)	
5.5/1 (2.3)	
6/10 (22.4)	
8/1 (2.3)	
9/4 (9.1)	
12/14 (31.8)	
SSTR2A positive total	38 (86.4%)
IRS SSTR3	IRS classification SSTR3
Score/frequency (%)	Score/frequency (%)
0/2 (4.5)	0/2 (4.5)
2/2 (4.5)	1/3 (6.8)
3/2 (4.5)	2/33 (75)
4/11 (25)	3/6 (13.6)
4.5/2 (4.5)	
5.5/1 (2.3)	
6/9 (20.5)	
8/8 (18.2)	
9/3 (6.8)	
12/3 (6.8)	
SSTR3 positive total	39 (88.6%)
IRS SSTR4	IRS classification SSTR4
Score/frequency (%)	Score/frequency (%)
0/1 (2.3)	0/1 (2.3)
2/3 (6.8)	1/21 (47.7)
2.5/2 (4.5)	2/22 (50)
3/11 (25)	
3.5/5 (11.4)	
4/14 (31.8)	
6/4 (9.1)	
8/4 (9.1)	
SSTR4 positive total	22 (50%)

Table 3 (continued)

IRS SSTR-subtype	IRS classification SSTR-subtype
IRS SSTR5	IRS classification SSTR5
Score/frequency (%)	Score/frequency (%)
0/8 (18.2)	0/10 (22.7)
1/2 (4.5)	1/14 (31.8)
2/9 (20.5)	2/20 (45.5)
3/3 (6.8)	
3.5/2 (4.5)	
4/11 (25)	
4.5/1 (2.3)	
6/6 (13.6)	
8/2 (4.5)	
SSTR5 positive total	20 (45.5%)

SSTR PET/CT. For the first time, a correlation between the SSTR expression pattern of all SSTR subtypes and the SUV in SSTR PET/CT using the peptide DOTA-NOC was possible.

Limitations

One limitation of this study was its retrospective nature, which may have caused incomplete and inaccurate documentation. Another limitation was seen in the semi-quantitative immunohistochemical analysis of the tissue sections, which was subjective and thereby limited the comparability.

Frequency of the SSTR subtypes

The predominant SSTR subtypes in the immunohistochemical analysis were SSTR2A (86.4%) and SSTR3 (88.6%). The frequency of positivity for SSTR1, SSTR4 and SSTR5 was between 45 and 50%. Whereas SSTR1 and SSTR3–SSTR5 showed cytoplasmic staining, the immunoreaction of SSTR2A was membrane bound. The difference between cytoplasmic (SSTR1, SSTR3, SSTR5) and membrane-bound immunoreactions (SSTR2A) was already described by Kulaksiz et al. [5] and Zamora et al. [12]. An expression of SSTR in 80–100% has been reported in several studies of Reubi et al. [13, 14]. In an immunohistochemical analysis in 94 patients with GEP-NET by Zamora et al. of the five SSTR subtypes, SSTR2A dominated with an incidence of over 80%. In another immunohistochemical investigation by Kulaksiz et al. SSTR2A was found to be present in 86% as in our study [5, 12]. These findings support our result of a predominant expression of SSTR2A. What was surprising was the finding of a high incidence of SSTR3 in our survey. Whereas Papotti et al. [15] showed a comparable incidence of 60% in tumour samples from 15 patients with GEP-NET and Kulaksiz et al. [5] showed a commonness of 71%, Zamora et al. [12] reported about 26% and Reubi and Waser 2003 [16] described a much lesser incidence of SSTR3 with 15% as a result of a study being that of patients with only ileum NET. In the study of Zamora et al. with an incidence of 71%, there was a noticeably high presence of SSTR3 among the pancreatic NET, compared with the non-pancreatic NET. The high proportion of pancreatic NET in our study (35.3%) could therefore be an explanation for the high incidence of SSTR3. Also SSTR4 was surprisingly high in our evaluation, with an incidence of 50%. Its frequency has been described as marginal (<15%) in previous studies [4, 15–17]. The presence of SSTR1 (48 and 50%) and SSTR5 (46 and 52%) in our study are on the other hand comparable to the findings of Reubi and Waser [16] and Zamora et al. [12]. Papotti et al. and Kulaksiz et al. described a much higher frequency of SSTR5 (up to 83%) than in our investigation [5, 15]. While discussing the findings of our project in comparison with those of other researchers, it is essential to be aware of divergent methods for analysing expression of SSTR. Application of diverse antibodies in the analysis of SSTR expression with autoradiography and immunohistochemistry makes it difficult to compare results. The use of a uniform score for SSTR-evaluation is not yet noticeable. When looking at the score distribution of the IRS for SSTR3, there was an accumulation in the middle domain. The domain 3 (positive, high expression) was reached only by a small fraction (13.6%) compared to SSTR2A (40.9%), which would be supported by the findings of Reubi and Waser and Zamora et al. [12, 16]. The findings in our study may indicate that the applied antibody is more sensitive towards expression of the middle IRS domain of SSTR3. Such a result would certainly have an impact on future diagnostic and therapeutic strategies. Another reason for the accumulation in the middle IRS domain for SSTR3 could be a high false-positive rate or an incorrect definition of the value, which recognizes a tumour as positive. However, the antibodies have been repeatedly tested both by our group as well as by other investigators in various tumour tissues, so that a high false-positive rate seems rather unlikely [3, 5, 18–21].

Expression pattern of the SSTR subtypes

In IRS, the predominant combinations were SSTR2A and SSTR3 and further SSTR1, SSTR2A, SSTR3 and SSTR5. In 81.8% at least SSTR2A and SSTR3 were expressed and in 70.5% at least three subtypes were positive. A remarkable observation was that no tumour sample was negative for all SSTR subtypes in the IRS system.

However, different studies report about negative staining of SSTR. This observation has already been described by Papotti et al., who reported an incidence of totally negative cases in 7% [15]. In the immunohistochemical analysis of Zamora et al. [12] only 6% of the samples were negative for all subtypes, supporting the findings of Reubi et al., who reported that 82% of all analysed GEP-NET were positive for SSTR, using autoradiography for the subtypes 1–3 in their analyses [4, 22]. Furthermore, the findings of Reubi et al. indicate a simultaneous expression of different SSTR subtypes, as seen in our study. According to Reubi et al. NET can express at least three SSTR subtypes (1, 2A and 3) [13, 17]. Papotti et al. could even show that 90% of NET are positive for at least three subtypes [15]. Based on the findings of Reubi et al., the simultaneous expression of SSTR1 and SSTR3 is not likely to be found, supporting the findings in our study. The most commonly expressed subtypes in GEP-NET are known to be SSTR2A and SSTR5. Looking at the studies discussed above the findings of our study support the already known expression patterns of the SSTR subtypes and indicate the need for a thorough analysis of the specific expression pattern of a given NET, beyond the predominant incidence of SSTR2A, in order to enable effective diagnostics and therapy of NET.

Chromogranin A and synaptophysin

Chromogranin A and synaptophysin staining were both positive in 82.4% of the patients, respectively. The observation that the IRS and IRS classification of SSTR2A correlated positively ($p<0.01$) with the degree of the chromogranin A staining was surprising. A mild positive staining never showed a positive SSTR2A expression and a negative chromogranin A staining resulted in a maximum IRS only once. This specific sample had offered problems in the analysis, because of its atypically dispersed tumour cells in the pancreatic capsule. No tumour cells were identified within the pancreatic tissue. Even though a correlation between chromogranin A concentration in plasma and a high percentage of positive chromogranin A staining has already been described in GEP-NET, a correlation between the SSTR2A expression and the chromogranin A staining has not yet been reported. This finding is, however, supported by the findings of Reubi et al., who could demonstrate that the intensity of the SSTR expression is linked to a high degree of differentiation of GEP-NET [23]. Also the findings of Stivanello et al., who demonstrated a significant correlation between well-differentiated NET and a high concentration of chromogranin A in plasma, support our results [24]. If, however, the correlation between chromogranin A and SSTR2A could be reproduced and confirmed in further studies with

more patients involved, conclusions about the SSTR2A receptor status could be made by routinely analysing the chromogranin A staining.

Grading

Tumour tissue with G2 grading was found in 53.7% of the patients, G1 grading in 17.1% and G3 grading in 29.3% of the patients. There was a significant inverse correlation between the grading and the IRS classification for SSTR2A. Tumour tissue with G3 grading had a lower incidence of SSTR2A than tumour with G1 or G2 grading. The degree of grading of the tumour tissue was therefore shown to have an influence on the SSTR2A status. A similar phenomenon has been described in other studies. Zamora et al. could show that well-differentiated tumours have a higher density and a more homogeneous distribution of SSTR (except for SSTR5) than lesser differentiated tumours [12]. Buscail et al. reported a similar observation for SSTR2A in pancreatic and colorectal tumours [25]. Papotti et al. also described an inverse correlation between SSTR2A expression and the degree of grading [15]. Tumours with a low degree of differentiation had a reduced incidence of SSTR; 60% of the tumours with a low degree of differentiation did not express any or only one SSTR. In comparison 12% of the tumours with a high degree of differentiation expressed SSTR. Reubi et al. described this phenomenon too, most of the SSTR-negative carcinoids belonged to an atypical category of carcinoids with a low degree of differentiation [13, 26]. Even though our findings are supported by already published results, it is important to recognize the uneven distribution of the individual degrees of grading, by which G2 was the dominant one with 64.7% prevalence. Still, the results confirm the hypothesis that the loss of SSTR expression leads to a benefit in growth and may be an explanation for the therapeutic ineffectiveness of somatostatin analogues in this tumour entity.

SSTR status and PET/CT calculations

The immunohistochemical scores of SSTR1, SSTR3 and SSTR4 did not show any significant correlation with the variable SUV_{max}. In contrast, a highly significant correlation was shown between SUV_{max} and the IRS of SSTR2A ($p<0.001$) and the IRS of SSTR5 ($p=0.038$). This could not be shown for the IRS classification of the two subtypes. SUV_{mean} correlated significantly with the IRS of SSTR2A ($p=0.013$). However, there was no significant correlation between SUV_{mean} and the scores of SSTR3, SSTR4 and SSTR5. Among the presently available SSTR analogues, ^{68}Ga-labelled DOTA-NOC offers the best affinity profile for the SSTR subtypes. There are several studies dealing with the affinity profiles of SSTR analogues and PET

tracers [6, 9, 27]. There is only one known investigation examining the correlation between the immunohistochemical SSTR status and SUV [28]. In this study by Miederer et al. the SUV of preoperative ^{68}Ga-DOTA-TOC PET/CT scans of 18 NET patients were correlated with an immunohistochemical score (0+ to 3+) for SSTR2A. NET with values of 2+ and 3+ resulted in a significantly higher SUV than NET with 0+ or 1+ [28]. Also SSTR5 correlated with SUV_{max}. Because the IC_{50} of ^{68}Ga-DOTA-NOC for SSTR5 is below 10 nmol/l, this result appears reasonable [9]. Despite the low IC_{50} of SSTR3 compared to the other SSTR analogues, the affinity (IC_{50}=40 nmol/l) does not seem high enough to result in a detection in the PET/CT. There was a correlation between SUV_{mean} and the IRS of SSTR2A in our study as well as in the study by Miederer et al. [28]. Both studies propose using SSTR2A immunohistochemistry in patients missing a preoperative PET scan and indicate SSTR PET/CT as a method for restaging and follow-up.

This study offers details about a differentiated individual-specific expression pattern of SSTR in GEP-NET, with varying density and intensity. The spectrum of expression patterns of SSTR with 16 different combinations is extensive. That at least three subtypes are present in over 70% of the cases and 81% contain SSTR2A and SSTR3, combined with the fact that there was no case of subtype-lacking, reflects the increasing importance of SSTR in the diagnostics and therapy of GEP-NET. The finding of a high frequency of expression of SSTR3 and SSTR4 gives a reason for reassessment of the present practice in diagnostics and therapy of GEP-NET, which primarily concentrates on SSTR2A. In further studies, specific expression patterns should be correlated with the response to therapy. The aim would be to define a selection of patients with an appropriate receptor profile based on immunohistochemical analysis, which would benefit from therapy with somatostatin analogues as well as PRRT.

Conclusion

Somatostatin receptor imaging with ^{68}Ga-DOTA-NOC PET/CT confirms histological conclusions with regard to therapy with somatostatin analogues, follow-up imaging as well as radionuclide therapy. The highly significant correlation between SSTR2A and SSTR5 and the SUV_{max} of the ^{68}Ga-DOTA-NOC PET/CT scans is concordant with the affinity profile of ^{68}Ga-DOTA-NOC to the SSTR subtypes and demonstrates the excellent qualification of somatostatin analogues in the diagnostics of NET.

References

1. Reubi JC. Somatostatin and other peptide receptors as tools for tumor diagnosis and treatment. Neuroendocrinology 2004;80 Suppl 1:51–6.
2. Taniyama Y, Suzuki T, Mikami Y, Moriya T, Satomi S, Sasano H. Systemic distribution of somatostatin receptor subtypes in human: an immunohistochemical study. Endocr J 2005;52:605–11.
3. Fischer T, Doll C, Jacobs S, Kolodziej A, Stumm R, Schulz S. Reassessment of sst2 somatostatin receptor expression in human normal and neoplastic tissues using the novel rabbit monoclonal antibody UMB-1. J Clin Endocrinol Metab 2008;93:4519–24.
4. Reubi JC. Peptide receptors as molecular targets for cancer diagnosis and treatment. Endocr Rev 2003;24:389–427.
5. Kulaksiz H, Eissele R, Rössler D, Schulz S, Höllt V, Cetin Y, et al. Identification of somatostatin receptor subtypes 1, 2A, 3, and 5 in neuroendocrine tumours with subtype specific antibodies. Gut 2002;50:52–60.
6. Reubi JC, Schär JC, Waser B, Wenger S, Heppeler A, Schmitt JS, et al. Affinity profiles for human somatostatin receptor subtypes SST1-SST5 of somatostatin radiotracers selected for scintigraphic and radiotherapeutic use. Eur J Nucl Med 2000;27:273–82.
7. Rufini V, Calcagni ML, Baum RP. Imaging of neuroendocrine tumors. Semin Nucl Med 2006;36:228–47.
8. Hofmann M, Maecke H, Börner R, Weckesser E, Schöffski P, Oei L, et al. Biokinetics and imaging with the somatostatin receptor PET radioligand (68)Ga-DOTATOC: preliminary data. Eur J Nucl Med 2001;28:1751–7.
9. Antunes P, Ginj M, Zhang H, Waser B, Baum RP, Reubi JC, et al. Are radiogallium-labelled DOTA-conjugated somatostatin analogues superior to those labelled with other radiometals? Eur J Nucl Med Mol Imaging 2007;34:982–93.
10. Forrer F, Riedweg I, Maecke HR, Mueller-Brand J. Radiolabeled DOTATOC in patients with advanced paraganglioma and pheochromocytoma. Q J Nucl Med Mol Imaging 2008;52:334–40.
11. McCarty Jr KS, Miller LS, Cox EB, Konrath J, McCarty Sr KS. Estrogen receptor analyses. Correlation of biochemical and immunohistochemical methods using monoclonal antireceptor antibodies. Arch Pathol Lab Med 1985;109:716–21.
12. Zamora V, Cabanne A, Salanova R, Bestani C, Domenichini E, Marmissolle F, et al. Immunohistochemical expression of somatostatin receptors in digestive endocrine tumours. Dig Liver Dis 2010;42:220–5

13. Reubi JC, Laissue J, Waser B, Horisberger U, Schaer JC. Expression of somatostatin receptors in normal, inflamed, and neoplastic human gastrointestinal tissues. Ann N Y Acad Sci 1994;733:122–37.

14. Reubi JC, Waser B, van Hagen M, Lamberts SW, Krenning EP, Gebbers JO, et al. In vitro and in vivo detection of somatostatin receptors in human malignant lymphomas. Int J Cancer 1992;50:895–900.

15. Papotti M, Bongiovanni M, Volante M, Allia E, Landolfi S, Helboe L, et al. Expression of somatostatin receptor types 1–5 in 81 cases of gastrointestinal and pancreatic endocrine tumors. A correlative immunohistochemical and reverse-transcriptase polymerase chain reaction analysis. Virchows Arch 2002;440:461–75.

16. Reubi JC, Waser B. Concomitant expression of several peptide receptors in neuroendocrine tumours: molecular basis for in vivo multireceptor tumour targeting. Eur J Nucl Med Mol Imaging 2003;30:781–93.

17. Reubi JC, Waser B, Schaer JC, Laissue JA. Somatostatin receptor sst1-sst5 expression in normal and neoplastic human tissues using receptor autoradiography with subtype-selective ligands. Eur J Nucl Med 2001;28:836–46.

18. Schulz S, Schmidt H, Händel M, Schreff M, Höllt V. Differential distribution of alternatively spliced somatostatin receptor 2 isoforms (sst2A and sst2B) in rat spinal cord. Neurosci Lett 1998;257:37–40.

19. Schulz S, Schreff M, Schmidt H, Händel M, Przewlocki R, Höllt V. Immunocytochemical localization of somatostatin receptor sst2A in the rat spinal cord and dorsal root ganglia. Eur J Neurosci 1998;10:3700–8.

20. Schulz S, Schulz S, Schmitt J, Wiborny D, Schmidt H, Olbricht S, et al. Immunocytochemical detection of somatostatin receptors sst1, sst2A, sst2B, and sst3 in paraffin-embedded breast cancer tissue using subtype-specific antibodies. Clin Cancer Res 1998;4:2047–52.

21. Thodou E, Kontogeorgos G, Theodossiou D, Pateraki M. Mapping of somatostatin receptor types in GH or/and PRL producing pituitary adenomas. J Clin Pathol 2006;59:274–9.

22. Reubi JC. Peptide receptor expression in GEP-NET. Virchows Arch 2007;451 Suppl 1:S47–50.

23. Reubi JC, Krenning E, Lamberts SW, Kvols L. Somatostatin receptors in malignant tissues. J Steroid Biochem Mol Biol 1990;37:1073–7.

24. Stivanello M, Berruti A, Torta M, Termine A, Tampellini M, Gorzegno G, et al. Circulating chromogranin A in the assessment of patients with neuroendocrine tumours. A single institution experience. Ann Oncol 2001;12 Suppl 2:S73–7.

25. Buscail L, Saint-Laurent N, Chastre E, Vaillant JC, Gespach C, Capella G, et al. Loss of sst2 somatostatin receptor gene expression in human pancreatic and colorectal cancer. Cancer Res 1996;56:1823–7.

26. Reubi JC, Schaer JC, Waser B, Mengod G. Expression and localization of somatostatin receptor SSTR1, SSTR2, and SSTR3 messenger RNAs in primary human tumors using in situ hybridization. Cancer Res 1994;54:3455–9.

27. Wild D, Schmitt JS, Ginj M, Macke HR, Bernard BF, Krenning E, et al. DOTA-NOC, a high-affinity ligand of somatostatin receptor subtypes 2, 3 and 5 for labelling with various radiometals. Eur J Nucl Med Mol Imaging 2003;30:1338–47.

28. Miederer M, Seidl S, Buck A, Scheidhauer K, Wester HJ, Schwaiger M, et al. Correlation of immunohistopathological expression of somatostatin receptor 2 with standardised uptake values in 68Ga-DOTATOC PET/CT. Eur J Nucl Med Mol Imaging 2009;36:48–52.